Algal Research 79 (2024) 103461

Contents lists available at ScienceDirect

Algal Research

journal homepage: www.elsevier.com/locate/algal

Temperature effects on growth, metabolome, lipidic profile and photosynthetic pigment content of *Microglena antarctica* (chlorophyceae): A comprehensive analysis

Riccardo Trentin [a], Emanuela Moschin [a], Luísa Custódio [b], Isabella Moro [a,c,*]

[a] Department of Biology, University of Padova, Via U. Bassi 58/B, 35131 Padova, Italy
[b] Centre of Marine Sciences, Faculty of Sciences and Technology, University of Algarve, Ed. 7, Campus of Gambelas, 8005–139 Faro, Portugal
[c] Department of Integrative Marine Ecology, Stazione Zoologica Anton Dohrn, Villa Comunale, 80121 Napoli, Italy

ARTICLE INFO

Keywords:
Antarctic microalgae
Untargeted metabolomics
Fatty acids profile
Photosynthetic pigment content
Growth curves
Temperature stress

ABSTRACT

Antarctic microalgae have evolved a wide range of adaptations to survive at extreme environmental conditions. This study aimed to explore the physiological and biochemical processes occurring in *Microglena antarctica* (Chlorophyceae) in response to changes in temperature. *M. antarctica* cultivated at three distinct temperatures (4 °C, 8 °C and 16 °C) exhibited variations in growth patterns, metabolomes, fatty acid methyl esters (FAMEs) profile and photosynthetic pigment concentrations. Our results highlighted a decrease in growth at 16 °C, confirming the cryophilic nature of this species. The growth rates at the exponential phase were observed to decrease progressively with an initial rate of (0.29 ± 0.05 d^{-1}) at the culturing temperature of 4 °C, followed by 8 °C (0.24 ± 0.09 d^{-1}), and further reduction at 16 °C (0.16 ± 0.05 d^{-1}). An integrative untargeted metabolomics approach combining mass spectral libraries and novel *in–silico* tools was employed to improve feature annotation and to provide additional information on features chemical classes. Significant differences in *M. antarctica* annotated compounds, chemical classes and whole metabolomes were observed among 4, 8 and 16 °C. Finally, targeted analyses were performed to evaluate changes in lipid profiles and photosynthetic pigment content. Higher percentages of polyunsaturated fatty acids (PUFAs) were observed at 4 and 8 °C, approximately 65.00 % of total FAMEs, and decreased to 60.71 % at 16 °C. Monounsaturated fatty acids (MUFAs) significantly increased at 16 °C, reaching up to 10.96 % of total FAMEs, in contrast to 4 °C and 8 °C, where the content of MUFAs was around 5.00 %. Additionally, chlorophyll *a* and carotenoid content increased by 50–100 % at 16 °C compared to lower temperatures. The present work highlights temperature–related responses in *M. antarctica* biochemical profile, combining untargeted and targeted approaches, and physiology, by growth analysis.

1. Introduction

Microalgae are important contributors to primary productivity in alpine and polar regions representing a key element in polar food webs and playing a crucial role in global carbon fixation [1–4]. Despite their important ecological functions in cold ecosystems, many aspects related to their biology, diversity and physiological and biochemical adaptations remain largely unknown [5]. Most of these algae are psychrophilic organisms growing efficiently at cold temperatures (~0 °C), but with a limited growth and survival capacity at moderate temperatures (~20 °C) [6,7]. Their inability to survive at moderate temperatures renders these organisms very sensitive to climate change. Cold ecosystems at high latitude [8] and altitudes [9] are experiencing particularly rapid climatic changes with several possible consequences on primary producers and, therefore, on species at higher trophic levels and carbon cycle [10]. In this sense, the study of psychrophilic algae will serve as an important biological indicator for evaluating the effects of environmental changes worldwide [1,11]. Up to date, about 100 species of psychrophilic algal species spread across several eukaryotic lineages have been classified [1,2,12] suggesting psychrophily as a trait acquired multiple times and independently in different phyla or as an ancestral character [2]. More than a third of microalgae adapted to cold environmental conditions belong to the Chlamydomonadales order (Chlorophyta, Reichenbach) and are spread into four main clades: '*Desmotetra*', '*Chloromonadinia*', '*Moewusinia*' and '*Monadinia*' [2,5,13–23]. Two cryophilic species of the '*Desmotetra*–clade', namely *Desmotetra*

* Corresponding author at: Department of Biology, University of Padova, Via U. Bassi 58/B, 35131 Padova, Italy.
E-mail address: imoro@bio.unipd.it (I. Moro).

https://doi.org/10.1016/j.algal.2024.103461
Received 6 November 2023; Received in revised form 26 February 2024; Accepted 2 March 2024
Available online 4 March 2024

aureospora Ling and *D. antarctica* (Fritsch) Ling were isolated from Windmill Islands in continental Antarctica, habitats characterized by high pH, around 6.8 and 7.8, and conductivity conditions, among 279 $\mu S \cdot cm^{-1}$ and 426 $\mu S \cdot cm^{-1}$, suggesting unusual adaptations to cope with these stressors [17]. '*Chloromonadinia*–clade' includes several lineages of psychrophiles found in polar and alpine snowfields [24] responsible for seasonal blooms known as 'red snow' [25] for the abundance in these species of red secondary pigments, such as astaxanthin [3]. *Chlamydomonas raudensis* Ettl, known also as *Chlamydomonas priscuii* [26], but currently not taxonomically accepted, is the unique lineage of obligate psychrophiles within the '*Moewusinia*–clade' [13] and it is considered an emerging model for cold adaptation of photosynthesis [1]. Similarly, *Microglena antarctica* Trentin, Negrisolo, Moschin, Veronese, Cecchetto & I.Moro is the only species with a formal identification belonging to the 'polar–clade' within the genus *Microglena* Ehrenberg *emend.* Demchenko, Mikhailyuk & Pröschold, formerly known as '*Monadinia*–clade' [5,18]. This alga is a marine psychrophilic microorganism adapted to extreme salt fluctuations [5,27], temperatures and light conditions, and its genome sequencing is providing significant improvements for the elucidations of the genetic basis of these adaptations [28]. *Microglena antarctica* and closely related species, are widely distributed in sea–ice, constituting up 99 % of the species composition of green snow [29], in the water column of Antarctic lakes and Southern Ocean [28,30]. *M. antarctica* is considered an emerging model organism for the study of algal adaptations to extreme environments and an important component in sea–ice communities [28]. Thus, for its ecological importance, wide distribution, cultivation feasibility and availability of reference literature for comparisons *M. antarctica* represent a valuable species for the understanding of the biochemical adaptation to temperature of polar microalgae [27,31,32]. Despite the genomes of some psychrophilic microalgae have been recently sequenced, information on their metabolomes is scarce [1,2]. In the last decades, several research focused on the study of specific chemical class, in particular lipids, heat shock proteins (HSPs) and photosynthetic pigments, as a response to extreme environmental stressors [1,2]. However, other compound families might be involved in adaptations to cold environments.

In the present study, we aimed to investigate the physiological and metabolic responses of *Microglena antarctica* IMA076A, isolated from Inexpressible Island (Terra Nova Bay, Ross Sea, Antarctica) to three different temperatures, ranging from 4 to 16 °C. At first, cell growth was evaluated under different temperatures. Secondly, an untargeted metabolomics approach, coupling liquid chromatography (LC) with high resolution tandem mass spectrometry (MS/MS), was employed to study the chemical differences induced by temperature variations in the whole algal metabolome and unravel new potential biomarkers for temperature. To cope with the limited information regarding marine compounds in mass spectral libraries, we used novel *in–silico* tools to better understand the 'chemical dark matter' [33,34] in *M. antarctica* metabolome. The combination of traditional MS/MS library search with *in–silico* analyses provided novel data regarding the chemical classes changes in temperature–related responses. Ultimately, targeted analyses of lipid profiles and photosynthetic pigment content were carried out to corroborate the information retrieved with LC–MS and to compare our results with previous findings in closely related psychrophilic phototrophs. The main objective of the present study is to explore the physiological and biochemical responses of the polar alga *M. antarctica* to different temperature, aiming to understand the evolution of psychrophily in Antarctic phototrophs. These data are of utmost importance considering current environmental changes that are threatening Antarctica. Robust evidence on the effect of stressor in polar algae may contribute to the existing set of indicators and assist in guiding effective ecosystem management, essential for maintaining the biodiversity, productivity, and resilience of Antarctic ecosystems and communities.

2. Materials and methods

2.1. Culture set up and growth curve

M. antarctica IMA076A was grown in triplicate with a F/2 medium [35] at three different temperatures, 4°, 8° and 16 °C, with a continuous light intensity of 35 μmol photons m^{-2} s^{-1}, to simulate the environmental parameters of the Antarctic summer, after an acclimatation period of 10 days at each experimental condition. For each temperature, inocula of *M. antarctica* IMA076A were started with a cell density of 25 × 10^3 cells ml^{-1}. Microalgal growth was evaluated by cell counting using a Neubauer chamber until the stationary phase. Cell densities were expressed as mean ± standard deviation (SD) of those obtained in three independent experiments. The growth rate of *M. antarctica* IMA076A was calculated using the equation:

$$\mu = ln(N_2/N_1)/(t_2 - t_1) \quad (1)$$

where:

μ = growth rate (d^{-1}).

N_1 and N_2 are the cell densities at time 1 (t_1) and time 2 (t_2), corresponding to beginning and ending of a growth phase.

2.2. Metabolomics

2.2.1. Extract preparation

Microalgal biomass was harvested at the end of exponential growth phase (day 14) by centrifugation and immediately frozen with liquid nitrogen. Freeze–dried biomass was obtained upon lyophilization for 24 h and stored at room temperature (RT) in the dark. Acetone extracts were prepared by mixing freeze–dried biomass of *M. antarctica* (50 mg) with 20 mL of 80 % (*v*/v) acetone. Subsequently, the algal cell walls were disrupted with glass beads in a MM400 mixer mill (Retsch, Haan, Germany) at 30 Hz for 5 min. After 12 h of incubation at 4 °C, they were centrifuged at 12,000*g* for 10 min at 4 °C and the supernatants were collected, filtered (0.2 μm) and diluted at the concentration of 2 mg/mL for the determination of their chemical profiles. A quality control (QC) sample was prepared by mixing equal volumes of each filtered extract.

2.2.2. UPLC–HR–MS/MS data acquisition

The chemical profiles of *M. antarctica* IMA076A extracts at 4, 8 and 16 °C were analyzed in triplicates by liquid chromatography–high resolution mass spectrometry (LC–HR–MS) following Silva et al. [36]. The extracts were analyzed using a Thermo Scientific™ UltiMate™ 3000 UHPLC coupled with an Orbitrap Elite (Thermo Fisher Scientific, Waltham, MA, USA) mass spectrometer equipped with a Heated Electro–Spray Ionization source (HESI–II; Thermo Scientific). The extracts (5 μL, 1:10 diluted in LC–MS grade methanol) were injected and separated with a Thermo Scientific Accucore RP–18 column (2.1 × 100 mm, 2.6 μm) on a 40 min run. The mobile phase consisted of ultra–pure LC–MS grade water with 0.1 % formic acid and LC–MS grade acetonitrile, containing 0.1 % formic acid. Positive polarity data were acquired. Extracts were analyzed in data–dependent mode with the selection of the three most intense ions under dynamic exclusion and collision–induced dissociation (CID) activation. MS/MS fragmentation was achieved using 35 keV rising collision energy in an isolation window of 2. The minimum signal required for ddMS2 triggering was 1000. Xcalibur v4.1 Qual Browser (Thermo Scientific, Waltham, MA, USA) was used for LC–MS data acquisition and subsequent analyses. Thermo ".raw" data files were converted to ".mzXML" format in centroid mode using Proteowizard [37]. The mass spectrometry data are deposited on the Mass Spectrometry Interactive Virtual Environment (MassIVE) repository (massive.ucsd.edu) with accession number MSV000092740 and are publicly available.

2.2.3. Feature finding and annotation of MS/MS spectra

Proteowizard ".mzXML" output files were imported in MZmine version 3.2.3 [38] for feature finding, alignment and extraction (parameters listed in Supplementary Materials Table S10). Feature intensities were assessed as the peak area in the extracted ion chromatogram (XIC). Blank was used for background feature removal and final features were exported as ".mgf" and ".csv" files. Features were analyzed in Global Natural Products Social Molecular Networking [39] (GNPS; http://gnps.ucsd.edu, accessed on 6 June 2022) platform for analysis with the Molecular–Library Search–V2 tool (workflow version release_28). Search parameters were reported in Supplementary Materials Table S11. In parallel, Thermo ".raw" data were processed in Compound Discoverer™ 3.2.0.421 (Thermo Fisher Scientific, Waltham, MA, USA). Untargeted metabolomics workflow (Untargeted Metabolomics with Statistics Detect Unknowns with ID Using Online Databases and mzLogic) was used to perform features alignment and unknown compound annotation using publicly available databases. The "Detect Unknown Compounds" node parameters used default values, except for mass tolerance (set to 10 [ppm]) and minimum peak intensity (set to 1000). The "Search ChemSpider" node was used to search spectral libraries by using Natural Products Atlas [40], Lipid Maps [41], KEGG [42], Drugbank [43] and BioCyc [44] databases. Blank was used for background feature removal and final features were exported as a ".csv" file. Features retrieved with MZmine 3 and Compound Discoverer were manually checked and merged.

2.2.4. In–silico annotation

SIRIUS 5 [45] was used to assign features molecular formulas and predict their structures and chemical classes based on the fragmentation patterns in MS/MS spectra and the MS1 (parent ion) isotope patterns [46]. Within the workflow, ZODIAC [47], CSI:FingerID [48], and CANOPUS based on ClassyFire ChemOnt ontology [49,50] tools were employed.

Following parameters were used: for SIRIUS: instrument profile (orbitrap), MS1 isotope pattern filter (true), MS2 mass accuracy (10 ppm), MS/MS isotope scorer (IGNORE), candidates stored (10), number of candidates per ion (1), consider only formulas in DBs (none), possible ionizations ([M + H]+, [M + K]+ and [M + Na]+), tree timeout (0), compound timeout (0), use heuristic above *m/z* (300), use heuristic only above *m/z* (650), formula settings enforced (HCNOP), formula settings detectable (B, Cl, Br, Se, S); for ZODIAC: considered candidates at 300 *m/z* (10), considered candidates at 800 *m/z* (50), use two–steps approach (true), edge threshold (0.995), min local connections (10), iterations (20000), burn–in (2000), separate runs (10); for CSI:FingerID: fallback adducts ([M + Na]+, [M + H]+, [M + K]+), score threshold (true), structure search DB (all). Following the workflow reported by Koester et al. [34], we only considered for subsequent analyses those features displaying: 1) a ZODIAC score above 0.98 and 2) a CANOPUS class probability above 0.2.

2.2.5. Final feature annotation

Identification levels were based on the convention reported in Sumner et al. [51]. However, in this work, a conservative approach was employed for final feature annotation. Features were assigned to level 2 when displaying congruent annotations using both library spectral match and *in–silico* fragmentation tools. When a feature showed different spectral library and *in–silico* annotation, it was assigned to the annotation level 3. Features that did not reach the required ZODIAC score and/or CANOPUS probability were considered as level 4.

2.3. Fatty acid methyl esters (FAME) profiling

2.3.1. Fatty acid transesterification

Lipids and free fatty acids (FA) were converted to their corresponding fatty acid methyl ester (FAME), by direct transesterification using acetyl chloride/methanol, followed by extraction of the lipidic phase into hexane according to the method described by Lepage and Roy with modifications [52,53]. In brief, lyophilized algal biomass (100 mg) was mixed with 1.5 mL of the derivatization solution (methanol/acetyl chloride, 20:1, *v*/v), and homogenized in an ultrasound–water bath for 30 min, at room temperature (RT). Afterwards, 1 mL of hexane was added to the samples and heated at 100 °C for 60 min. After cooling in an ice bath, 1 mL of distilled water was added, and samples were centrifuged for 5 min at 5000*g*. The supernatants were collected, filtered (0.2 μm) and used for the determination of FAMEs profile [28]. FAMEs extractions were performed in triplicates.

2.3.2. FAME profiling by gas chromatography–mass spectrometry (GC–MS)

The FAME profiles of *M. antarctica* IMA076A biomass were analyzed by an Agilent GC–MS (Agilent Technologies 6890 Network GC System, 5973 Inert Mass Selective Detector) coupled with a ZB–5MS capillary column (30 m × 0.25 mm internal diameter, 0.25 μm film thickness, Agilent Tech) using helium as the carrier gas. Samples were injected at 300 °C and the temperature profile of the GC oven was 60 °C (1 min), 30 °C/min to 120 °C, 4 °C/min to 250 °C, and 20 °C/min to 300 °C (4 min). For the identification of FAMEs, the total ion mode was used and Supelco® 37 Component FAME Mix (Sigma-Aldrich, Sintra, Portugal) was used as standard. Values were expressed as percentages of total FAMEs.

2.4. Pigment analysis

For the measurement of chlorophyll *a* (Chl *a*), chlorophyll *b* (Chl *b*) and total carotenoid (Tot car) contents, freeze–dried biomass (~100 mg) was mixed with 80 % acetone (1 mL) and cells were disrupted with glass beads (425–600 μm) in a MM400 mixer mill (Retsch, Haan, Germany). After 12 h of incubation at 4 °C, the absorbance (A_x) of the supernatant was measured at 664, 647, 630, 510 and 480 nm by a UV–visible spectrophotometer (Genesys 50, Thermo Scientific). The pigment concentrations, expressed as mg g^{-1} dry weight (DW), were estimated using the following equations [54]:

$$\text{Chl } a = (12.21 \text{ x } A_{663} - 2.81 \text{ x } A_{646})/W)*(V/1000) \quad (2)$$

$$\text{Chl } b = (20.13 \text{ x } A_{646} - 2.03 \text{ x } A_{663})/W)*(V/1000) \quad (3)$$

$$\text{Tot car} = \{[(1000 \text{ x A470} - 3.27 \text{ x Chl } a - 104 \text{ x Chl } b)/198]/W\}*(V/1000) \quad (4)$$

where:

W = sample weight (g of fresh weight)
V = 80 % acetone volume (mL)
A_{664}, A_{647}, A_{630}, A_{480}, A_{510} = absorbance at *x* nm.

2.5. Statistical analysis

Statistical analyses were performed in R–Statistics® 3.2.3 version. Cell growth data were analyzed using one–way ANOVA, followed by a Tukey's post–hoc tests with multiple comparisons to highlight statistical differences in growth at different temperatures. Metabolomics data were analyzed through different steps (multivariate and univariate). After blank removal, features relative abundances were normalized to ensure gaussian distribution. At first, PERMANOVA tests (n permutation = 999) and PCoA visualization were performed based on Canberra distances to examine sample clustering using "vegan" and "ggplot2" R packages. Major variations in the data were explained by PCoA axes. To visualize the relative variation of the discriminating features across different samples, normalized data were analyzed with the "pheatmap" package as summarized in a heatmap. Four additional R packages ("ggsci", "matrixStats", "ggrepel" and "tidyverse") were employed to investigate differences in the levels of individual features between different

temperatures in the dataset using ANOVA followed by Tukey's post hoc test. Finally, PERMANOVA tests (n permutation = 999) and PCA visualization based on Euclidean distances were used to evaluate differences among major chemical classes. FAMEs profile and pigment content results were compared by one–way ANOVA, followed by a post–hoc test (Tukey's test).

3. Results

3.1. Growth of Microglena antarctica

M. antarctica was grown in batch cultures exposed to three different temperatures respectively 4°, 8° and 16 °C. In all cultures, growth kinetic was monitored following the increase in cell density, as reported in Fig. 1. One–way ANOVA analysis highlighted a statistically significant effect of temperature on cell growth of *M. antarctica*. From day 0 to day 6, no significant differences were observed between the cell densities of *M. antarctica* grown at 4°, 8° and 16 °C (Supplementary Materials Table S1). At day 8, cultures grown at 4 °C showed lower cell densities compared to cultures grown at 8 °C (p–value < 0.05). From day 12 to day 16, the cell densities of 16 °C cultures were significantly lower than cultures at 4° and 8 °C (Supplementary Materials Table S1). No significant differences in the growth rates were reported among cultures cultivated at 4°, 8° and 16 °C during lag phase (Fig. 2), when the growth rates were $0.07 \pm 0.05\ d^{-1}$ at 4 °C, $0.03 \pm 0.07\ d^{-1}$ at 8 °C and $0.08 \pm 0.04\ d^{-1}$ at 16 °C. Statistical differences were reported among treatments during the exponential growth phase, when *M. antarctica* showed the highest growth rate ($0.29 \pm 0.05\ d^{-1}$) at the culturing temperature of 4 °C, followed by 8 °C ($0.24 \pm 0.09\ d^{-1}$) and 16 °C ($0.16 \pm 0.05\ d^{-1}$).

3.2. Chemical profiling

3.2.1. Metabolomic analysis

The metabolomic profiles of *M. antarctica* acetone extracts recovered from biomass grown at three different temperatures (4°, 8° and 16 °C) were determined through an untargeted UPLC–HR–MS/MS approach. A principal coordinate analysis (PCoA) based on complete metabolic profiles of *M. antarctica* (Fig. 3) highlighted temperature–related clustering of the biological replicates. The 48.4 % of the variance among replicates was accounted by the first coordinate (PCoA 1) which separated *M. antarctica* 4 °C metabolome to 8 °C and 16 °C metabolomes, while 8 °C and 16 °C metabolomes were mainly differentiated along the second coordinate (PCoA 2, 32.5 %). These results evidenced distinct metabolic signatures related to growth temperature as supported by a PERMANOVA analysis (p–value < 0.05, Supplementary Materials Table S2).

To identify the temperature–dependent metabolic features in *M. antarctica* cultivated at 4 °C, 8 °C and 16 °C, whole metabolome samples were examined in triplicates. Out of the 708 features obtained in this experiment, 250 features (35 % of the total) were not significantly different between the cultures (ANOVA, Benjamini–Hochberg adjusted p–value > 0.05) and 9 had spectral matches with compounds reposited in libraries. The remaining 458 features (65 % of the total) displayed significant differences (ANOVA, Benjamini–Hochberg adjusted p–value

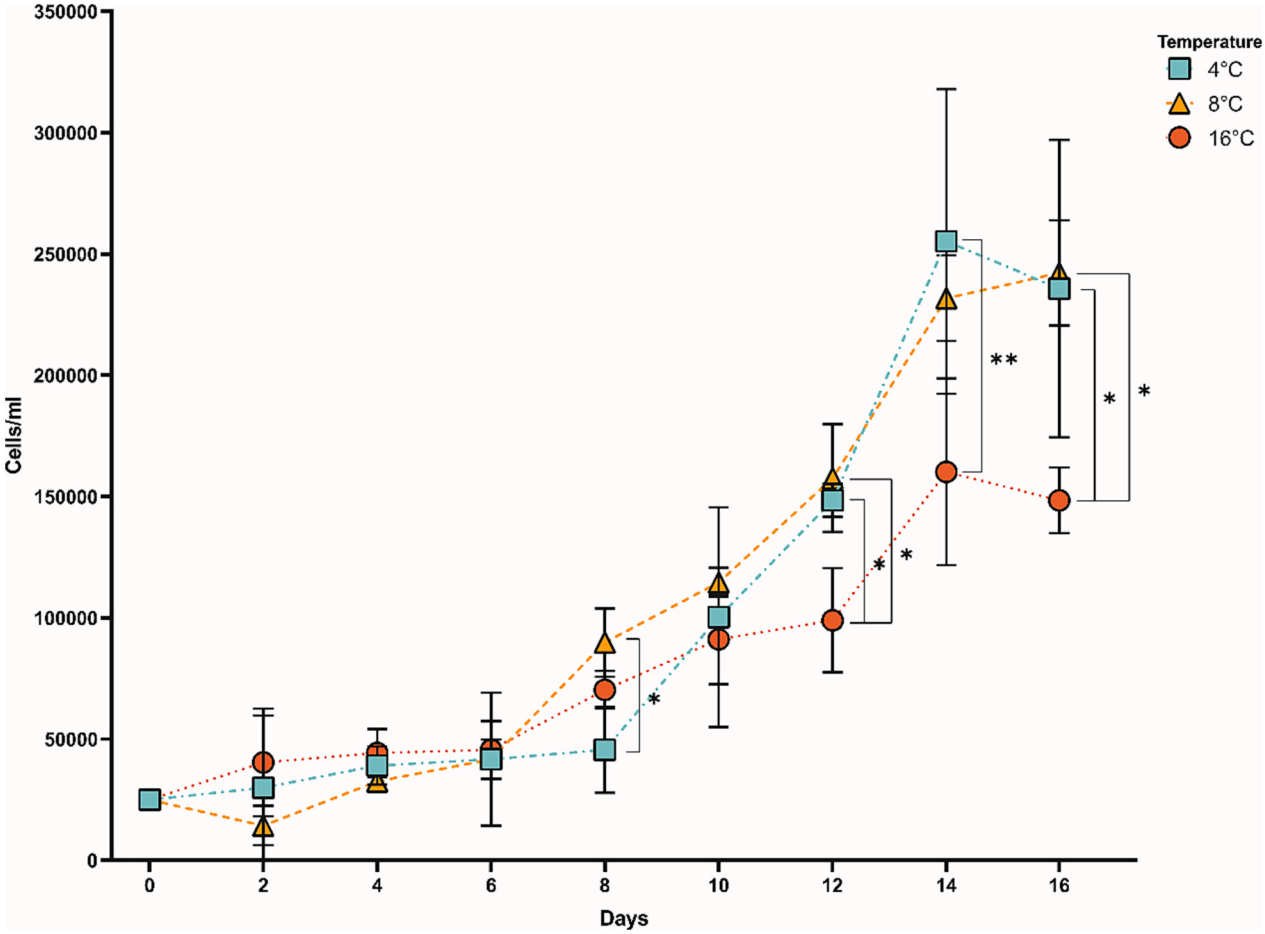

Fig. 1. Growth curves of *M. antarctica* under different temperatures. Blue squares, 4 °C; orange triangles, 8 °C; red circles, 16 °C. Asterisks indicate statistically significant differences ('***' = p–value < 0.001; '**' = p–value < 0.01 and '*' = p–value < 0.05). (For interpretation of the references to color in this figure legend, the reader is referred to the web version of this article.)

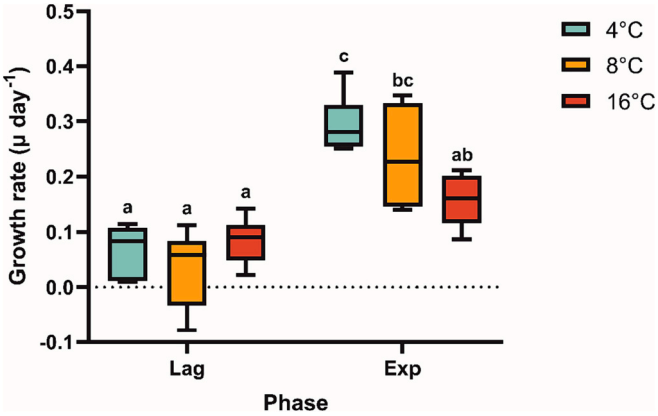

Fig. 2. Growth rate of *M. antarctica* at 4 °C (blue), 8 °C (orange) and 16 °C (red) within lag (Lag) and exponential (Exp) phases. The letters above the boxplots indicate significantly different groups (Multiple Comparisons of Means: Tukey's HSD, 95 % family-wise confidence level). (For interpretation of the references to color in this figure legend, the reader is referred to the web version of this article.)

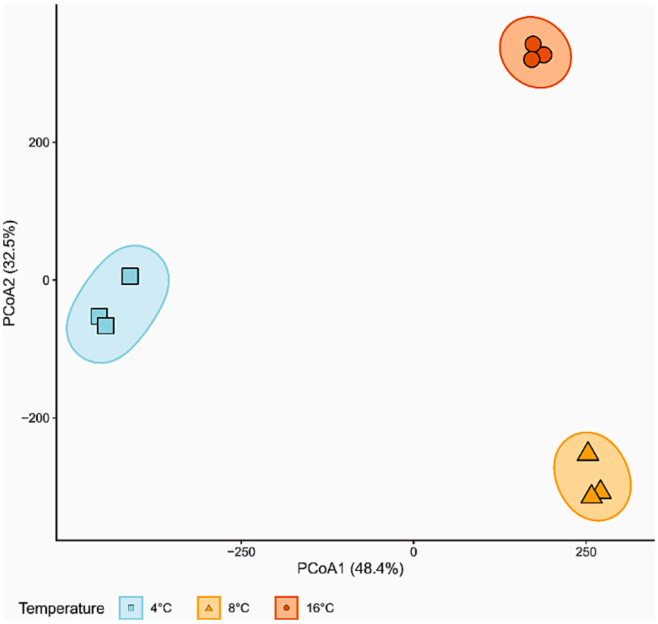

Fig. 3. Principal coordinate analysis (PCoA) of metabolomic profiles of *M. antarctica* color coded by the three different temperatures (4°, 8° and 16 °C). The x– and y–axes represent principal coordinates 1 and 2, respectively, in brackets the percentages of the overall variance explained by each principal coordinate. PERMANOVA analysis proved distinct metabolomes at different temperatures (p–value < 0.05). Blue squares, 4 °C; orange triangles, 8 °C; red circles, 16 °C. (For interpretation of the references to color in this figure legend, the reader is referred to the web version of this article.)

< 0.05). Library spectral matches allowed the annotation as putative compound of 104 features (level 2), while *in–silico* approach resulted in the chemical class prediction of 156 features (level 3). Level 2 annotated features showing statistical variations at different temperatures were visualized through a hierarchical clustering heatmap (Fig. 4).

The main chemical classes identified in *M. antarctica* metabolome included lipids and lipid–like molecules, such as fatty acyls (36 % of the features identified at class level), glycerolipids (34 %), steroids and steroid derivatives (9 %) and prenol lipids (5 %), organoheterocyclic compounds, such as tetrapyrroles and derivatives (8 %) and organic acids and derivatives, such as carboxylic acids and derivatives (5 %). Principal component analyses (PCA) of single chemical subclasses (Fig. 5a–k) resulted in discrimination of the samples into three groups according to growth temperature. The observed discrimination was validated using a permutation test (Supplementary Materials Table S2), confirming significant effects of temperature on most chemical subclasses (PERMANOVA, p–value < 0.05). Among glycerolipids, monoradylglycerols, diradylglycerols, triradylcglycerols, glycosylmonoradylglycerols and glycosyldiacylglycerols showed different temperature–related changes (Fig. 5a–e). However, fatty acyls subclasses, fatty acids and conjugates, fatty amides and lineolic acids and derivatives, showed a very similar trend of change in this experiment (Fig. 5f–h). With the increase of the temperature, unsaturated octadecanoids, such as parinaric acid (C18:4), alpha–linolenic acid (C18:3), linoleamide (NA 18:2), linoleic and rumenic acids (C18:2) decreased in abundance (p–value > 0.05, Supplementary Materials Tables S3–S7). Amino acids, peptides, and analogues (Fig. 5i) at 8° and 16 °C clustered closer compared to those annotated at 4 °C. A significant increase in xanthophylls and chlorophyll derivatives (chlorins) was observed in at higher temperatures (p–value >0.05, Supplementary Materials Tables S3–S7) and confirmed by similar clustering by PCA plotting (Fig. 5j–k).

3.2.2. *FAMEs profiling*

The FAMEs profile of *M. antarctica* comprised six compounds (Fig. 6). The most abundant FAME was 9,12–octadecadienoic acid FAME (C18:2), followed by methyl palmitate (C16:0) and 9–octadecenoic acid methyl ester (C18:1). These proportions remained constant across all growth temperatures. Methyl laurate (C12:0), methyl palmitoleate (C16:1) and 9–octadecenoic acid methyl ester (C18:1) exhibited significantly higher levels at 16 °C, while methyl palmitate (C18:0) and 9,12–octadecadienoic acid fatty acid methyl ester (C18:2) showed increased abundance at 4 °C and 8 °C. No statistically significant differences were observed in methyl stearate content among the tested temperatures. Polyunsaturated fatty acids (PUFAs) were the most abundant FAMEs, followed by saturated (SFAs) and monounsaturated (MUFAs) fatty acids (Fig. 7). At 4 and 8 °C, PUFAs were significantly higher than 16 °C, while MUFAs were significantly lower. SFAs percentages were constant among different temperature treatments (Supplementary Materials Tables S8–S10).

3.2.3. *Pigment analysis*

Chlorophyll and total carotenoid contents (Fig. 8) were measured at the end of the exponential growth phase (day 14). Cells grown at 16 °C showed the highest concentration of photosynthetic pigments. Statistically significant differences were observed between 16 °C and both 4 °C and 8 °C for chlorophyll *a* (Chl *a*), while carotenoid content was significantly lower at 4 °C compared to 16 °C. No statistical differences were observed for chlorophyll *b* (Chl *b*) among different temperatures (Supplementary Materials Tables S11–S12).

4. Discussion

In this work, *M. antarctica* cultures grown at three different temperatures (4°, 8° and 16 °C) showed differences in growth, metabolomes, FAMEs profiles and photosynthetic pigment concentrations. Our results indicate that 4° and 8 °C were the optimal growth temperatures in terms of biomass production, with a significantly higher cell density compared to cells cultivated at 16 °C. These results are consistent with those reported for *M. antarctica* ICE–L (former *Chlamydomonas* sp. ICE–L), where the optimum growth temperature ranged from 4° to 10 °C [21] and with the phylogenetic related *Chlamydomonas* sp. ARC isolated from Chukchi sea ice, where the maximum growth rate was found at 5 °C [22].

The chemical diversity of *M. antarctica* metabolomes under three different temperatures was initially explored by an untargeted approach. Out of a total of 708 features identified, a mere 15 % of features was successfully matched to existing compound libraries, which is

Fig. 4. Hierarchical clustering analysis of temperature distinguishing features, indicated as feature ID followed by putative compound name. Colors from blue to yellow indicate the normalized relative abundance values of metabolites from low to high according to the scale bar. Samples of *M. antarctica* grown at 4 °C (blue), 8 °C (orange) and 16 °C (red) are disposed in columns; replicates are indicated with the strain code (IMA076A) followed by the temperature (4, 8 or 16 °C) and the suffix number (1, 2 and 3). Feature chemical subclasses are indicated in different colors. (For interpretation of the references to color in this figure legend, the reader is referred to the web version of this article.)

typical for marine samples, indicating the limited coverage of available spectral references [34]. To gain insights into the remaining features, we employed an *in–silico* approach, which associated the 31 % of the detected features to a chemical class, significantly expanding our understanding of metabolomes composition of *M. antarctica*. Through a PCoA (Fig. 3) and a hierarchical clustering (Fig. 4), we highlighted distinct temperature–related clustering of *M. antarctica* metabolomes and we were able to visualize the distinguishing features chemical classes and intensity pattern across the samples. Differences in major chemical subclasses were summarized using PCA (Fig. 5). Remarkably, the PCA plots showed variations in all the most abundant chemical subclasses in response to changes in temperature. Multivariate statistical approach supported the significant effect of temperature on *M. antarctica* whole metabolome and on major compound subclasses (Supplementary Materials Table S2). Univariate statistical analysis was employed to study temperature effect on single features (Supplementary Materials Tables S3–S6 and Figs. S1–S5). This integrative untargeted metabolomics approach, combining both mass spectral libraries and novel *in–silico* tools, facilitated the annotation of features and chemical classes across cell cultures exposed to different temperatures. Moreover, it provided additional information regarding feature's chemical classes and subclasses that might serve as potential targets in future investigations, specifically as temperature biomarkers for Antarctic microalgae.

After observing significant differences in major features chemical classes through untargeted metabolomics analysis, we conducted targeted analysis to better understand the changes in lipid profiles (via GC–MS) and photosynthetic pigment content (using spectrophotometric analysis). In fact, alterations in fatty acids (FA) profiles [55] and photosynthetic pigment contents [56–58] are widely recognized biomarkers for the study of temperature–induced changes in microalgae. Changes in lipid content, FA profiles and degree of carbon chain saturation represent common adaptive responses to temperature variations [59–61]. In particular, the inverse correlation between growth temperature and PUFAs accumulation, common in algae and plants [59,62], is considered a mechanism for the maintenance of membrane fluidity and it is regulated by FA desaturases (FADs) [63]. A transcriptomic analysis of five FA desaturases (FADs) in *M. antarctica* ICE–L suggested differential gene expressions of four FADs in response to temperature stress and an alteration of the FA composition was confirmed by GC–MS analysis which highlighted a significant increase of PUFAs at 0 and 5 °C [32]. In our experiment, variations in the FAMEs profiles at different temperatures (Fig. 5) suggested a similar trend. Higher percentages of PUFAs were observed at 4 and 8 °C compared to cells grown at 16 °C (p–value < 0.001), while MUFAs showed an opposite trend significantly increasing at 16 °C. As reported in many plant and algal species, growth at elevated temperatures coincided with a decrease C18:2 fatty acids (FAs) and a corresponding increase in C18:1 FAs levels [62]. After

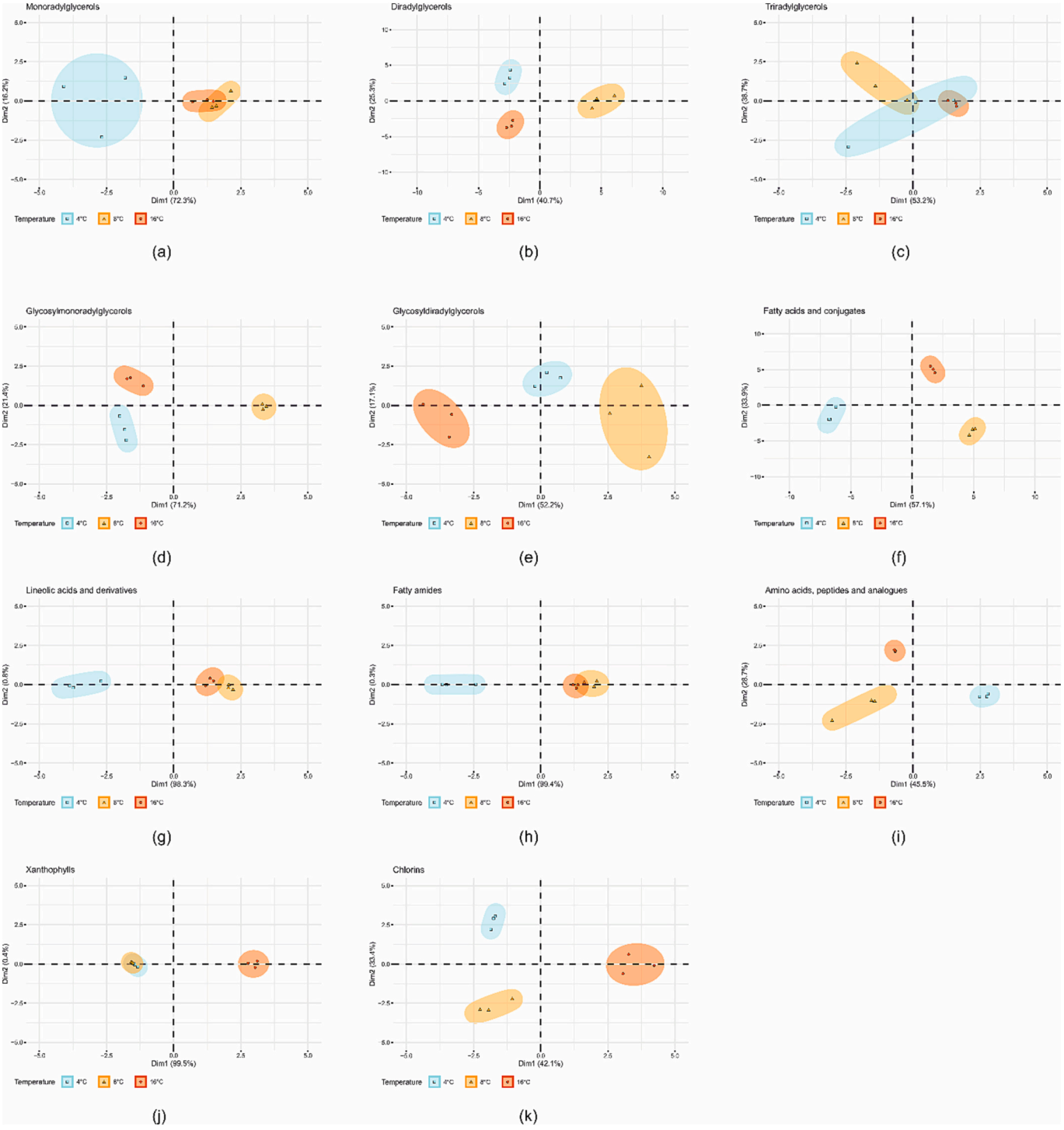

Fig. 5. Principal components analysis (PCA) showing the dissimilarities between *M. antarctica* metabolome at different temperatures in terms of: (a) monoradylglycerols; (b) diradylglycerols; (c) triradylcglycerols; (d) glycosylmonoradylglycerols; (e) glycosyldiacylglycerols; (f) fatty acids and conjugates; (g) fatty amides; (h) lineolic acids and derivatives; (i) amino acids, peptides, and analogues; (j) xanthophylls; (k) chlorins. The x– and y–axes represent principal components 1 and 2, respectively, in brackets the percentages of the overall variance explained by each principal component. Chemical profiles of three independent replicates were analyzed per temperature (4°, 8° and 16 °C). PERMANOVA analysis proved distinct metabolomes at different temperatures ($p < 0.05$).

short–time exposure of 2.5 h to low temperature (−25 °C), *M. antarctica* ICE–L decreased saturation level of C18 FAs [31]. Similarly, An et al. 2013 [32], reported considerably higher percentages of C18:3 at 0 and 5 °C. Despite the FAMEs profile of the phylogenetic related species *Chlamydomonas* sp. UMACC 229 from Antarctica was rich in PUFAs, an increase of PUFAs was reported between 4 and 14 °C (from 70.8 to 75.3 %), while a drop of PUFAs percentage was recorded only at 20 °C (65.7 %) [64]. Interestingly, differences in FAMEs profiles between *M. antarctica* IMA076A, *M. antarctica* ICE–L [31,32] and *Chlamydomonas* sp. UMACC 229 were observed [64]. *M. antarctica* ICE–L was rich in C18:3 FAMEs according to both Yi–Bin et al. 2017 [31] and An et al. [32], while C20:3 and C20:5 FAMEs were detected just by An et al. [32]. C16:3 was the dominant FAs in *Chlamydomonas* sp. UMACC 229, while C18:2 and C18:3 were relatively lower (~10 %) and C20:3 and C20:5

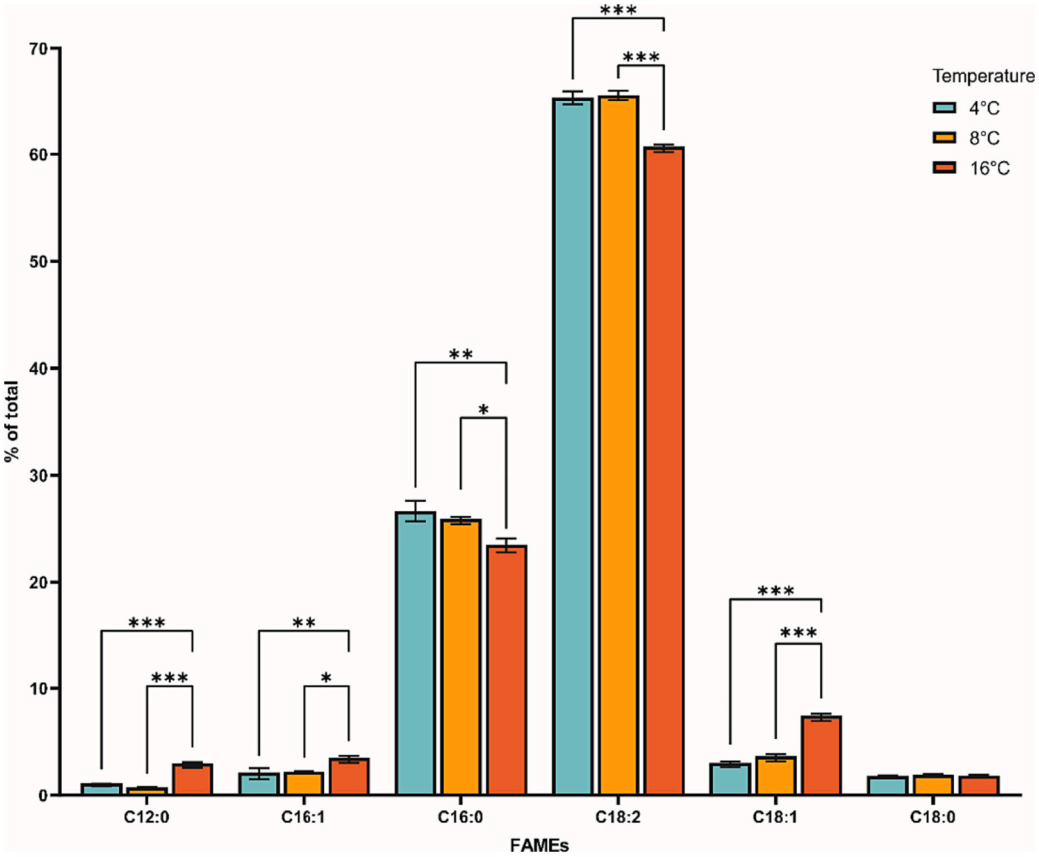

Fig. 6. FAMEs profile of *M. antarctica* at 4 °C (blue), 8 °C (orange) and 16 °C (red). Results are expressed as percentage of total FAMEs. Asterisks indicate statistically significant differences ('***' = p–value < 0.001; '**' = p–value < 0.01 and '*' = p–value < 0.05). (For interpretation of the references to color in this figure legend, the reader is referred to the web version of this article.)

FAMEs were not detected [64]. In *M. antarctica* IMA076A, C18:2 was the dominant FAMEs, while C18:3, C20:3 and C20:5 FAMEs were not identified. Differences in FAMEs profiles might be accounted by the growing conditions employed by the authors. While *Chlamydomonas* sp. UMACC 229 and *M. antarctica* ICE–L were grown in Provasoli seawater medium [65] with ~40 μmol photons m^{-2} s^{-1} on 12:12 h light–dark cycle by Teoh et al. [64] and An et al. [32], *M. antarctica* ICE–L was cultivated in the same medium and light–dark cycle, but with a lower light intensity of 20–30 μmol photons m^{-2} s^{-1} by Yi–Bin et al. 2016 [31]. To simulate real environmental conditions during Antarctic summer, *M. antarctica* IMA076A was grown in F/2 medium [12] at a continuous light intensity of 35 μmol photons m^{-2} s^{-1}. However, despite these differences in FAMEs profile, *M. antarctica* IMA076A, *Chlamydomonas* sp. UMACC 229 and *M. antarctica* ICE–L generally increased in PUFAs percentages to cope with low temperatures. Furthermore, LC–MS data showed that *M. antarctica* IMA076A features corresponding to PUFAs were statistically higher at 4 °C (Supplementary Materials Tables S3–S7).

Temperature is also considered a relevant stressor affecting photosynthetic pigment production [66]. For this reason, we measured chlorophyll and total carotenoid content in response to different cultivation temperatures. Chlorophyll *a* was the most abundant pigment in *M. antarctica* IMA076A, followed by chlorophyll *b* and carotenoids, as reported for *M. antarctica* ICE–L [31]. Our results indicated a significant increase in chlorophyll *a* and carotenoid concentrations at 16 °C. These results slightly differ from those reported for *M. antarctica* ICE–L [31]. In fact, while chlorophyll *b* was constant in both IMA076A and ICE–L strains, Yi–Bin et al. 2016 observed a decrease in chlorophyll *a* levels of *M. antarctica* ICE–L as a short–term response to cold temperature (24 h of exposure), followed by a slow increase after 32 h [31]. This late increase in chlorophyll *a*, if prolonged in time, might represent a possible mechanism of photosynthetic acclimation and end up to a long–term rise of chlorophyll *a*, as observed in IMA076A strain. Cold temperatures (between 10 and 20 °C) in the mesophilic green alga *C. reinhardtii*, a closely related species to *M. antarctica*, induced carotenoid and chlorophyll accumulation [67]. Interestingly, in this species, a sharp decrease in growth below 10 °C was observed. These results suggest an opposite response to temperature–related stress in mesophilic and cryophilic Chlamydomonadales, with the firsts decreasing in growth and accumulating photosynthetic pigments as response to cold, and the seconds reducing growth rate and increasing pigment content as response to heat. These variations in photosynthetic pigment asset might represent an additional survival strategy adopted by cryophilic Chlamydomonadales to cope with heat stress, which, together with the photosynthetic regulation promoted by excess light, could lead to their blooming in polar environment and Alps, as for *C. nivalis* [68]. In mesophilic Chlamydomonadales the increase of carotenoid levels might be involved in cold stress acclimation by changing the membrane fluidity [69]. Further studies are necessary to evaluate whether this mechanism is conserved as a physiological response of cryophilic Chlamydomonadales to extremely low temperatures. Napaumpaiporn and Sirikhachornkit studied the effect of high temperature on carotenoid accumulation in *C. reinhardtii* [70]. Their results showed that increasing growth temperature leads to chlorophyll and carotenoid accumulation in the presence of light [70]. However, while the importance of carotenoids for photoprotection in Chlamydomonadales is well–known, future research is required to understand the role of these pigments in heat stress. The increase of carotenoid content as a response to high cultivation temperatures was reported for other algal species, such as *Dunaliella salina* [71,72] and *Pavlova lutheri* [73], and it was considered

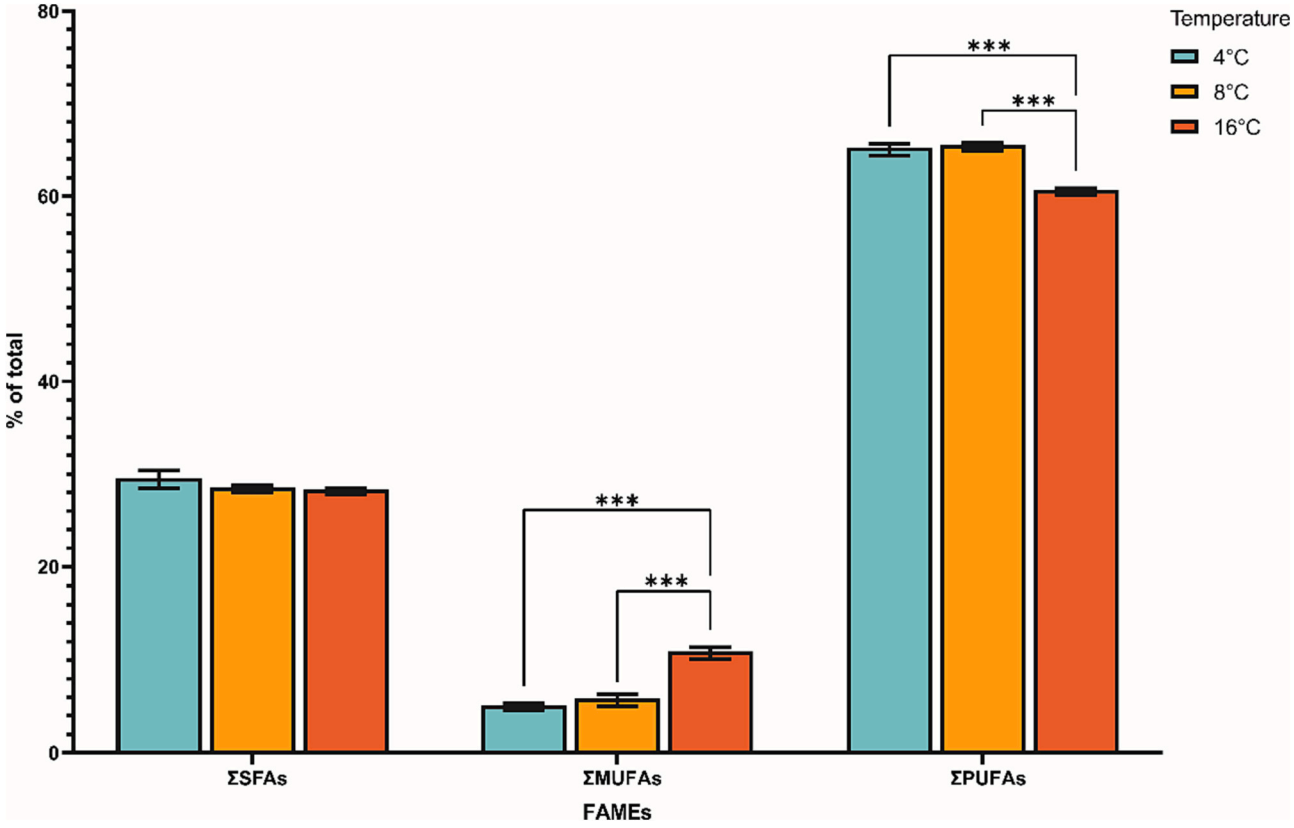

Fig. 7. Total saturated (ΣSFA), monounsaturated (ΣMUFA) and polyunsaturated (ΣPUFA) fatty acids of *M. antarctica* at 4 °C (blue), 8 °C (orange) and 16 °C (red). Results are expressed as percentage of total FAMEs. Asterisks indicate statistically significant differences ('***' = p–value < 0.001; '**' = p–value < 0.01 and '*' = p–value < 0.05). (For interpretation of the references to color in this figure legend, the reader is referred to the web version of this article.)

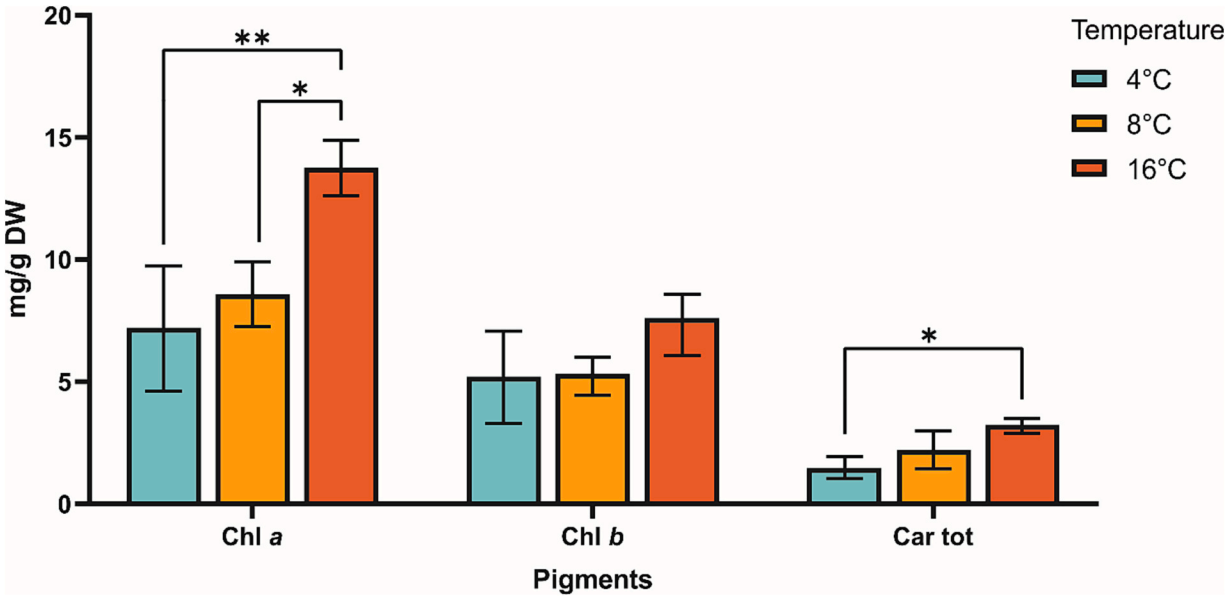

Fig. 8. Chlorophyll *a* (Chl *a*), chlorophyll *b* (Chl *b*) and total carotenoid (Car tot) content of *M. antarctica* at 4 °C (blue), 8 °C (orange) and 16 °C (red). Results are expressed as mg/g of dry weight (DW). Asterisks indicate statistically significant differences ('***' = p–value < 0.001; '**' = p–value < 0.01 and '*' = p–value < 0.05). (For interpretation of the references to color in this figure legend, the reader is referred to the web version of this article.)

as an adaptive strategy to reduce the formation of reactive oxygen species (ROS) during heat stress [68,70]. A similar mechanism could be used by *M. antarctica* IMA076A.

5. Conclusions

The present work is the first attempt to study *M. antarctica* response to different temperatures in terms of growth and biochemical composition, combining an untargeted metabolomics and a targeted analysis of

FAMEs and photosynthetic pigments. Our results confirmed *M. antarctica* as a psychrophilic microalga, with an optimal growth rate of $0.29 \pm 0.05\ d^{-1}$ at 4 °C and a reduction in growth at 8 °C ($0.24 \pm 0.09\ d^{-1}$) and 16 °C ($0.16 \pm 0.05\ d^{-1}$). Untargeted metabolomic approach annotated a small percentage of total features based on public spectral libraries. However, *in–silico* approach provided molecular formulas and compound class affiliations independently of spectral libraries, representing an important implementation of traditional MS/MS library search. This approach highlighted variations in the main chemical classes of *M. antarctica* metabolites, expanding the spectrum of potential biochemical alterations resulting from temperature changes in cryophilic microalgae. Specifically, glycerolipids and other lipid–like molecules showed significant variations, rendering these compounds as potential targets for future investigations into the temperature adaptation of polar algae. Thus, we recommend the use of an untargeted metabolomic strategy for the study of non–model algae and for the exploration of unknown metabolic responses. Our LC–MS data of *M. antarctica* metabolomes are publicly available for future re–analysis and represent a contribution in our understanding of algal metabolism under temperature stress. FAMEs analyses showed a significant increase in PUFAs at lower temperatures, supporting the hypothesis of their role in membrane fluidity. Finally, photosynthetic pigments increased as a response to high temperatures, suggesting an adaptive strategy to cope with heat stress. The survival capacity shown by *M. antarctica* up to 16 °C open interesting reflections on its evolutionary history and its responses in a changing environment. A major hypothesis for the evolution of psychrophily in algae, considers this process as a gradual increase in cold tolerance, allowing mesophilic species to survive to seasonal fluctuations of temperatures [2]. This have led to the loss of capacity to survive at moderate temperature values in some species (true psychrophiles), while many other Antarctic algae can survive above ambient polar temperatures [2]. It is important to underline that the capacity of *M. antarctica* to grow at non–polar temperatures does not consider the physiological state of the organism. For instance, while growth capacity at higher temperature in laboratory conditions might seem positive in the context of global warming concerns, other key cellular processes involving algal metabolism can be negatively affected, limiting *M. antarctica* survival in its natural environment. Further studies are necessary to clarify the effects of different temperature on cryophilic Chlamydomonadales.

Supplementary data to this article can be found online at https://doi.org/10.1016/j.algal.2024.103461.

CRediT authorship contribution statement

Riccardo Trentin: Writing – original draft, Visualization, Validation, Software, Methodology, Investigation, Formal analysis, Data curation, Conceptualization. **Emanuela Moschin:** Writing – review & editing, Validation, Investigation, Formal analysis, Data curation. **Luísa Custódio:** Writing – review & editing, Validation, Supervision, Resources, Methodology, Funding acquisition. **Isabella Moro:** Writing – review & editing, Validation, Supervision, Resources, Funding acquisition, Conceptualization.

Declaration of competing interest

The authors declare that they have no known competing financial interests or personal relationships that could have appeared to influence the work reported in this paper.

Data availability

Data will be made available on request.

Acknowledgements

We wish to thank Dr. José Paulo da Silva and Dr. Vera Gomes (Centre of Marine Sciences, Faculty of Sciences and Technology, University of Algarve, Ed. 7, Campus of Gambelas, 8005–139 Faro, Portugal) for their assistance respectively with the LC–MS and GC–MS analyses.

Declaration of generative AI in scientific writing

During the preparation of this work AI was not employed by the author(s).

Funding authors

This work was funded by Portuguese national funds from FCT—Foundation for Science and Technology through projects UIDB/04326/2020, UIDP/04326/2020 and LA/P/0101/2020. Luísa Custódio was supported by the FCT Scientific Employment Stimulus (CEECIND/00425/2017). Isabella Moro was supported by two PNRA projects, PNRA16_00120 – A1 and PNRA18_00078 – B2.

References

[1] M. Cvetkovska, G. Vakulenko, D.R. Smith, X. Zhang, N.P.A. Hüner, Temperature stress in psychrophilic green microalgae: Minireview, Physiol. Plant. 174 (2022) e13811, https://doi.org/10.1111/PPL.13811.
[2] M. Cvetkovska, N.P.A. Hüner, D.R. Smith, Chilling out: the evolution and diversification of psychrophilic algae with a focus on Chlamydomonadales, Polar Biol. 40 (2016) 1169–1184, https://doi.org/10.1007/S00300-016-2045-4.
[3] D. Remias, U. Lütz-Meindl, C. Lütz, Photosynthesis, pigments and ultrastructure of the alpine snow alga *Chlamydomonas nivalis*, Eur. J. Phycol. 40 (2006) 259–268, https://doi.org/10.1080/09670260500202148.
[4] D. Remias, M. Pichrtová, M. Pangratz, C. Lütz, A. Holzinger, Ecophysiology, secondary pigments and ultrastructure of *Chlainomonas* sp. (Chlorophyta) from the European Alps compared with *Chlamydomonas nivalis* forming red snow, FEMS Microbiol. Ecol. 92 (2016), https://doi.org/10.1093/FEMSEC/FIW030.
[5] R. Trentin, E. Negrisolo, E. Moschin, D. Veronese, M. Cecchetto, I. Moro, *Microglena antarctica* sp. nov. a new Antarctic green alga from inexpressible island (Terra Nova Bay, Ross Sea) revealed through an integrative approach, Diversity 14 (2022) 337, https://doi.org/10.3390/D14050337.
[6] M.L. Teoh, W.L. Chu, H. Marchant, S.M. Phang, Influence of culture temperature on the growth, biochemical composition and fatty acid profiles of six Antarctic microalgae, J. Appl. Phycol. 16 (2004) 421–430, https://doi.org/10.1007/S10811-004-5502-3.
[7] R.E.H. Smith, L.C. Stapleford, R.S. Ridings, The acclimated response of growth, photosynthesis, composition, and carbon balance to temperature in the psychrophilic ice diatom *Nitzschia seriata*, J. Phycol. 30 (1994) 8–16, https://doi.org/10.1111/J.0022-3646.1994.00008.X.
[8] J. Royles, H. Griffiths, Invited review: climate change impacts in polar regions: lessons from Antarctic moss bank archives, in: Glob Chang Biol, Blackwell Publishing Ltd, 2015, pp. 1041–1057, https://doi.org/10.1111/GCB.12774.
[9] T. Kohler, M. Giger, H. Hurni, C. Ott, U. Wiesmann, S. Wymann Von Dach, D. Maselli, Mountains and climate change: a global concern, Mt. Res. Dev. 30 (2010) 53–55, https://doi.org/10.1659/MRD-JOURNAL-D-09-00086.1.
[10] N.S. Steiner, W.W.L. Cheung, A.M. Cisneros-Montemayor, H. Drost, H. Hayashida, C. Hoover, J. Lam, T. Sou, U.R. Sumaila, P. Suprenand, T.C. Tai, D.L. VanderZwaag, Impacts of the changing ocean-sea ice system on the key forage fish arctic cod (*Boreogadus saida*) and subsistence fisheries in the Western Canadian arctic-evaluating linked climate, ecosystem and economic (CEE) models, Front. Mar. Sci. 6 (2019), https://doi.org/10.3389/FMARS.2019.00179/FULL.
[11] M.N. Gooseff, J.E. Barrett, B.J. Adams, P.T. Doran, A.G. Fountain, W.B. Lyons, D. M. McKnight, J.C. Priscu, E.R. Sokol, C. Takacs-Vesbach, M.L. Vandegehuchte, R. A. Virginia, D.H. Wall, Decadal ecosystem response to an anomalous melt season in a polar desert in Antarctica, Nat. Ecol. Evol. 1 (2017) 1334–1338, https://doi.org/10.1038/s41559-017-0253-0.
[12] M.D. Guiry, G.M. Guiry, Algaebase, World-Wide Electronic Publication, National University of Ireland, Galway, 2022. https://www.algaebase.org (accessed January 3, 2022).
[13] C. Lemieux, A.T. Vincent, A. Labarre, C. Otis, M. Turmel, Chloroplast phylogenomic analysis of chlorophyte green algae identifies a novel lineage sister to the Sphaeropleales (Chlorophyceae) Phylogenetics and phylogeography, BMC Evol. Biol. 15 (2015) 1–13, https://doi.org/10.1186/S12862-015-0544-5/FIGURES/4.
[14] S. Watanabe, S. Tsujimura, T. Misono, S. Nakamura, H. Inoue, *Hemiflagellochloris kazakhstanica* gen. et sp. nov.: a new coccoid green alga with flagella of considerably unequal lenghts from a saline irrigation land in Kazakhstan (Chlorophyceae, Chlorophyta)e, J. Phycol. 42 (2006) 696–706, https://doi.org/10.1111/J.1529-8817.2006.00214.X.

[15] M. Possmayer, R.K. Gupta, B. Szyszka-Mroz, D.P. Maxwell, M.A. Lachance, N.P. A. Hüner, D.R. Smith, Resolving the phylogenetic relationship between *Chlamydomonas* sp. UWO 241 and *Chlamydomonas raudensis* SAG 49.72 (Chlorophyceae) with nuclear and plastid DNA sequences, J. Phycol. 52 (2016) 305–310, https://doi.org/10.1111/JPY.12383.

[16] A.D. Temraleeva, Y.S. Bukin, Morphology, molecular phylogeny, and species delimitation within microalgal genera *Eubrownia*, *Spongiococcum*, and *Chlorococcum* (Chlorophyceae, Chlorophyta), S. Afr. J. Bot. 151 (2022) 396–409, https://doi.org/10.1016/J.SAJB.2022.10.030.

[17] H.U. Ling, Snow algae of Windmill islands, continental Antarctica: *Desmotetra aureospora*, sp. nov. and *D. antarctica*, comb. nov (Chlorophyta), J. Phycol. 37 (2001) 160–174, https://doi.org/10.1046/J.1529-8817.2001.037001160.X.

[18] E. Demchenko, T. Mikhailyuk, A.W. Coleman, T. Pröschold, Generic and species concepts in *Microglena* (previously the *Chlamydomonas monadina* group) revised using an integrative approach, Eur. J. Phycol. 47 (2012) 264–290, https://doi.org/10.1080/09670262.2012.678388.

[19] T. Nakada, S. Takahashi, M. Tomita, *Microglena redcarensis* sp. nov. (Volvocales, Chlorophyceae), a brackish water chlamydomonad with contractile vacuoles, Phycological, Res 66 (2018) 310–317, https://doi.org/10.1111/PRE.12330.

[20] T. Nakada, M. Tomita, Light microscopy and phylogenetic analyses of *Chlamydomonas* species (Volvocales, Chlorophyceae). II. Molecular phylogeny, secondary structure of ITS-2, cell morphology, and nomenclature of *Microglena opisthopyren*, and *M. media*, comb. nov, APG 65 (2014) 67–73, https://doi.org/10.18942/APG.KJ00009406722.

[21] C. Liu, X. Huang, X. Wang, X. Zhang, G. Li, C. Liu, X. Huang, X. Wang, X. Zhang, G. Li, Phylogenetic studies on two strains of Antarctic ice algae based on morphological and molecular characteristics, Phycologia 45 (2006) 190–198, https://doi.org/10.2216/03-88.1.

[22] B. Eddie, C. Krembs, S. Neuer, Characterization and growth response to temperature and salinity of psychrophilic, halotolerant *Chlamydomonas* sp. ARC isolated from Chukchi Sea ice, Mar. Ecol. Prog. Ser. 354 (2008) 107–117, https://doi.org/10.3354/MEPS07243.

[23] T. Pröschold, B. Marin, U.G. Schlösser, M. Melkonian, Molecular phylogeny and taxonomic revision of *Chlamydomonas* (Chlorophyta). I. Emendation of *Chlamydomonas* Ehrenberg and *Chloromonas* Gobi, and description of *Oogamochlamys* gen. nov. and *Lobochlamys* gen. nov, Protist 152 (2001) 265–300, https://doi.org/10.1078/1434-4610-00068.

[24] R. Matsuzaki, H. Kawai-Toyooka, Y. Hara, H. Nozaki, Revisiting the taxonomic significance of aplanozygote morphologies of two cosmopolitan snow species of the genus *Chloromonas* (Volvocales, Chlorophyceae), Phycologia 54 (2015) 491–502, https://doi.org/10.2216/15-33.1.

[25] R.W. Hoham, B. Duval, Microbial ecology of snow and freshwater ice with emphasis on snow algae, in: H.G. Jones, J.W. Pomeroy, D.A. Walker, R.W. Hoham (Eds.), Snow Ecology: An Interdisciplinary Examination of Snow-Covered Ecosystems, Cambridge University Press, Cambridge, 2001, pp. 168–228.

[26] S. Stahl-Rommel, I. Kalra, S. D'Silva, M.M. Hahn, D. Popson, M. Cvetkovska, R. M. Morgan-Kiss, Cyclic electron flow (CEF) and ascorbate pathway activity provide constitutive photoprotection for the photopsychrophile, *Chlamydomonas* sp. UWO 241 (renamed *Chlamydomonas priscuii*), Photosynth. Res. 151 (2022) 235–250, https://doi.org/10.1007/S11120-021-00877-5.

[27] M. An, S. Mou, X. Zhang, Z. Zheng, N. Ye, D. Wang, W. Zhang, J. Miao, Expression of fatty acid desaturase genes and fatty acid accumulation in *Chlamydomonas* sp. ICE-L under salt stress, Bioresour. Technol. 149 (2013) 77–83, https://doi.org/10.1016/J.BIORTECH.2013.09.027.

[28] Z. Zhang, C. Qu, K. Zhang, Y. He, X. Zhao, L. Yang, Z. Zheng, X. Ma, X. Wang, W. Wang, K. Wang, D. Li, L. Zhang, X. Zhang, D. Su, X. Chang, M. Zhou, D. Gao, W. Jiang, F. Leliaert, D. Bhattacharya, O. De Clerck, B. Zhong, J. Miao, Adaptation to extreme Antarctic environments revealed by the genome of a sea ice green alga, Curr. Biol. 30 (2020) 3330–3341.e7, https://doi.org/10.1016/j.cub.2020.06.029.

[29] S. Lutz, A.M. Anesio, K. Field, L.G. Benning, Integrated "omics", targeted metabolite and single-cell analyses of arctic snow algae functionality and adaptability, Front. Microbiol. 6 (2015) 170604, https://doi.org/10.3389/FMICB.2015.01323/BIBTEX.

[30] X. Zhang, M. Cvetkovska, R. Morgan-Kiss, N.P.A. Hüner, D.R. Smith, Draft genome sequence of the Antarctic green alga *Chlamydomonas* sp. UWO241, IScience 24 (2021) 102084, https://doi.org/10.1016/J.ISCI.2021.102084.

[31] W. Yi-Bin, L. Fang-Ming, Z. Xiu-Fang, Z. Ai-Jun, Z. Zhou, S. Cheng-Jun, M. Jin-Lai, Composition and regulation of thylakoid membrane of Antarctic ice microalgae *Chlamydomonas* sp. ICE-L in response to low-temperature environment stress, J. Mar. Biol. Assoc. U. K. 97 (2017) 1241–1249, https://doi.org/10.1017/S0025315416000588.

[32] M. An, S. Mou, X. Zhang, N. Ye, Z. Zheng, S. Cao, D. Xu, X. Fan, Y. Wang, J. Miao, Temperature regulates fatty acid desaturases at a transcriptional level and modulates the fatty acid profile in the Antarctic microalga *Chlamydomonas* sp. ICE-L, Bioresour. Technol. 134 (2013) 151–157, https://doi.org/10.1016/J.BIORTECH.2013.01.142.

[33] R.R. Da Silva, P.C. Dorrestein, R.A. Quinn, Illuminating the dark matter in metabolomics, Proc. Natl. Acad. Sci. U. S. A. 112 (2015) 12549–12550, https://doi.org/10.1073/PNAS.1516878112.

[34] I. Koester, Z.A. Quinlan, L.F. Nothias, M.E. White, A. Rabines, D. Petras, J. K. Brunson, K. Dührkop, M. Ludwig, S. Böcker, F. Azam, A.E. Allen, P.C. Dorrestein, L.I. Aluwihare, Illuminating the dark metabolome of *Pseudo-nitzschia*–microbiome associations, Environ. Microbiol. 24 (2022) 5408–5424, https://doi.org/10.1111/1462-2920.16242.

[35] R.R.L. Guillard, Culture of phytoplankton for feeding marine invertebrates, Cult. Mar. Invertebrate Anim. (1975) 29–60, https://doi.org/10.1007/978-1-4615-8714-9_3.

[36] S.G. Silva, P. Paula, J.P. da Silva, D. Mil-Homens, M.C. Teixeira, A.M. Fialho, R. Costa, T. Keller-Costa, Insights into the antimicrobial activities and metabolomes of *Aquimarina* (Flavobacteriaceae, Bacteroidetes) species from the rare marine biosphere, Mar. Drugs 20 (2022) 423, https://doi.org/10.3390/MD20070423.

[37] M.C. Chambers, B. MacLean, R. Burke, D. Amodei, D.L. Ruderman, S. Neumann, L. Gatto, B. Fischer, B. Pratt, J. Egertson, K. Hoff, D. Kessner, N. Tasman, N. Shulman, B. Frewen, T.A. Baker, M.Y. Brusniak, C. Paulse, D. Creasy, L. Flashner, K. Kani, C. Moulding, S.L. Seymour, L.M. Nuwaysir, B. Lefebvre, F. Kuhlmann, J. Roark, P. Rainer, S. Detlev, T. Hemenway, A. Huhmer, J. Langridge, B. Connolly, T. Chadick, K. Holly, J. Eckels, E.W. Deutsch, R. L. Moritz, J.E. Katz, D.B. Agus, M. MacCoss, D.L. Tabb, P. Mallick, A cross-platform toolkit for mass spectrometry and proteomics, Nat. Biotechnol. 30 (2012) 918–920, https://doi.org/10.1038/nbt.2377.

[38] R. Schmid, S. Heuckeroth, A. Korf, A. Smirnov, O. Myers, T.S. Dyrlund, R. Bushuiev, K.J. Murray, N. Hoffmann, M. Lu, A. Sarvepalli, Z. Zhang, M. Fleischauer, K. Dührkop, M. Wesner, S.J. Hoogstra, E. Rudt, O. Mokshyna, C. Brungs, K. Ponomarov, L. Mutabdžija, T. Damiani, C.J. Pudney, M. Earll, P. O. Helmer, T.R. Fallon, T. Schulze, A. Rivas-Ubach, A. Bilbao, H. Richter, L. F. Nothias, M. Wang, M. Orešič, J.K. Weng, S. Böcker, A. Jeibmann, H. Hayen, U. Karst, P.C. Dorrestein, D. Petras, X. Du, T. Pluskal, Integrative analysis of multimodal mass spectrometry data in MZmine 3, Nat. Biotechnol. 41 (2023) 447–449, https://doi.org/10.1038/s41587-023-01690-2.

[39] M. Wang, J.J. Carver, V.V. Phelan, L.M. Sanchez, N. Garg, Y. Peng, D.D. Nguyen, J. Watrous, C.A. Kapono, T. Luzzatto-Knaan, C. Porto, A. Bouslimani, A.V. Melnik, M.J. Meehan, W.T. Liu, M. Crüsemann, P.D. Boudreau, E. Esquenazi, M. Sandoval-Calderón, R.D. Kersten, L.A. Pace, R.A. Quinn, K.R. Duncan, C.C. Hsu, D.J. Floros, R.G. Gavilan, K. Kleigrewe, T. Northen, R.J. Dutton, D. Parrot, E.E. Carlson, B. Aigle, C.F. Michelsen, L. Jelsbak, C. Sohlenkamp, P. Pevzner, A. Edlund, J. McLean, J. Piel, B.T. Murphy, L. Gerwick, C.C. Liaw, Y.L. Yang, H.U. Humpf, M. Maansson, R.A. Keyzers, A.C. Sims, A.R. Johnson, A.M. Sidebottom, B.E. Sedio, A. Klitgaard, C.B. Larson, C.A.P. Boya, D. Torres-Mendoza, D.J. Gonzalez, D. B. Silva, L.M. Marques, D.P. Demarque, E. Pociute, E.C. O'Neill, E. Briand, E.J. N. Helfrich, E.A. Granatosky, E. Glukhov, F. Ryffel, H. Houson, H. Mohimani, J. J. Kharbush, Y. Zeng, J.A. Vorholt, K.L. Kurita, P. Charusanti, K.L. McPhail, K. F. Nielsen, L. Vuong, M. Elfeki, M.F. Traxler, N. Engene, N. Koyama, O.B. Vining, R. Baric, R.R. Silva, S.J. Mascuch, S. Tomasi, S. Jenkins, V. Macherla, T. Hoffman, V. Agarwal, P.G. Williams, J. Dai, R. Neupane, J. Gurr, A.M.C. Rodríguez, A. Lamsa, C. Zhang, K. Dorrestein, B.M. Duggan, J. Almaliti, P.M. Allard, P. Phapale, L.F. Nothias, T. Alexandrov, M. Litaudon, J.L. Wolfender, J.E. Kyle, T. O. Metz, T. Peryea, D.T. Nguyen, D. VanLeer, P. Shinn, A. Jadhav, R. Müller, K. M. Waters, W. Shi, X. Liu, L. Zhang, R. Knight, P.R. Jensen, B. Palsson, K. Pogliano, R.G. Linington, M. Gutiérrez, N.P. Lopes, W.H. Gerwick, B.S. Moore, P. C. Dorrestein, N. Bandeira, Sharing and community curation of mass spectrometry data with global natural products social molecular networking, Nat. Biotechnol. 34 (2016) 828–837, https://doi.org/10.1038/nbt.3597.

[40] J.A. Van Santen, E.F. Poynton, D. Iskakova, E. Mcmann, T.A. Alsup, T.N. Clark, C. H. Fergusson, D.P. Fewer, A.H. Hughes, C.A. Mccadden, J. Parra, S. Soldatou, J. D. Rudolf, E.M.L. Janssen, K.R. Duncan, R.G. Linington, The Natural Products Atlas 2.0: a database of microbially-derived natural products, Nucleic Acids Res. 50 (2022) D1317–D1323, https://doi.org/10.1093/NAR/GKAB941.

[41] M. Sud, E. Fahy, D. Cotter, A. Brown, E.A. Dennis, C.K. Glass, A.H. Merrill, R. C. Murphy, C.R.H. Raetz, D.W. Russell, S. Subramaniam, LMSD: LIPID MAPS structure database, Nucleic Acids Res. 35 (2007) D527–D532, https://doi.org/10.1093/NAR/GKL838.

[42] M. Kanehisa, S. Goto, KEGG: Kyoto encyclopedia of genes and genomes, Nucleic Acids Res. 28 (2000) 27–30, https://doi.org/10.1093/NAR/28.1.27.

[43] D.S. Wishart, Y.D. Feunang, A.C. Guo, E.J. Lo, A. Marcu, J.R. Grant, T. Sajed, D. Johnson, C. Li, Z. Sayeeda, N. Assempour, I. Iynkkaran, Y. Liu, A. MacIejewski, N. Gale, A. Wilson, L. Chin, R. Cummings, Di. Le, A. Pon, C. Knox, M. Wilson, DrugBank 5.0: a major update to the DrugBank database for 2018, Nucleic Acids Res. 46 (2018) D1074–D1082, https://doi.org/10.1093/NAR/GKX1037.

[44] R. Caspi, T. Altman, R. Billington, K. Dreher, H. Foerster, C.A. Fulcher, T. A. Holland, I.M. Keseler, A. Kothari, A. Kubo, M. Krummenacker, M. Latendresse, L. A. Mueller, Q. Ong, S. Paley, P. Subhraveti, D.S. Weaver, D. Weerasinghe, P. Zhang, P.D. Karp, The MetaCyc database of metabolic pathways and enzymes and the BioCyc collection of pathway/genome databases, Nucleic Acids Res. 42 (2014) D459–D471, https://doi.org/10.1093/NAR/GKT1103.

[45] K. Dührkop, M. Fleischauer, M. Ludwig, A.A. Aksenov, A.V. Melnik, M. Meusel, P. C. Dorrestein, J. Rousu, S. Böcker, SIRIUS 4: a rapid tool for turning tandem mass spectra into metabolite structure information, Nat. Methods 16 (2019) 299–302, https://doi.org/10.1038/s41592-019-0344-8.

[46] S. Böcker, M.C. Letzel, Z. Lipták, A. Pervukhin, SIRIUS: decomposing isotope patterns for metabolite identification, Bioinformatics 25 (2009) 218–224, https://doi.org/10.1093/BIOINFORMATICS/BTN603.

[47] M. Ludwig, L.F. Nothias, K. Dührkop, I. Koester, M. Fleischauer, M.A. Hoffmann, D. Petras, F. Vargas, M. Morsy, L. Aluwihare, P.C. Dorrestein, S. Böcker, Database-independent molecular formula annotation using Gibbs sampling through ZODIAC, Nat. Mach. Intell. 2 (2020) 629–641, https://doi.org/10.1038/s42256-020-00234-6.

[48] M.A. Hoffmann, L.-F. Nothias, M. Ludwig, M. Fleischauer, E.C. Gentry, M. Witting, P.C. Dorrestein, K. Dührkop, S. Böcker, Assigning confidence to structural

annotations from mass spectra with COSMIC, BioRxiv (2021), https://doi.org/10.1101/2021.03.18.435634.
[49] K. Dührkop, L.F. Nothias, M. Fleischauer, R. Reher, M. Ludwig, M.A. Hoffmann, D. Petras, W.H. Gerwick, J. Rousu, P.C. Dorrestein, S. Böcker, Systematic classification of unknown metabolites using high-resolution fragmentation mass spectra, Nat. Biotechnol. 39 (2020) 462–471, https://doi.org/10.1038/s41587-020-0740-8.
[50] Y. Djoumbou Feunang, R. Eisner, C. Knox, L. Chepelev, J. Hastings, G. Owen, E. Fahy, C. Steinbeck, S. Subramanian, E. Bolton, R. Greiner, D.S. Wishart, ClassyFire: automated chemical classification with a comprehensive, computable taxonomy, J. Chem. 8 (2016) 1–20, https://doi.org/10.1186/S13321-016-0174-Y.
[51] L.W. Sumner, A. Amberg, D. Barrett, M.H. Beale, R. Beger, C.A. Daykin, T.W. M. Fan, O. Fiehn, R. Goodacre, J.L. Griffin, T. Hankemeier, N. Hardy, J. Harnly, R. Higashi, J. Kopka, A.N. Lane, J.C. Lindon, P. Marriott, A.W. Nicholls, M.D. Reily, J.J. Thaden, M.R. Viant, Proposed minimum reporting standards for chemical analysis: Chemical Analysis Working Group (CAWG) Metabolomics Standards Initiative (MSI), Metabolomics 3 (2007) 211–221, https://doi.org/10.1007/S11306-007-0082-2.
[52] G. Lepage, C.C. Roy, Improved recovery of fatty acid through direct transesterification without prior extraction or purification, J. Lipid Res. 25 (1984) 1391–1396.
[53] R. Trentin, L. Custódio, M.J. Rodrigues, E. Moschin, K. Sciuto, J.P. da Silva, I. Moro, Exploring Ulva australis Areschoug for possible biotechnological applications: in vitro antioxidant and enzymatic inhibitory properties, and fatty acids contents, Algal Res. 50 (2020) 101980, https://doi.org/10.1016/J.ALGAL.2020.101980.
[54] A.R. Wellburn, The spectral determination of chlorophylls a and b, as well as total carotenoids, using various solvents with spectrophotometers of different resolution, J. Plant Physiol. 144 (1994) 307–313, https://doi.org/10.1016/S0176-1617(11)81192-2.
[55] G.J.O. Martin, D.R.A. Hill, I.L.D. Olmstead, A. Bergamin, M.J. Shears, D.A. Dias, S. E. Kentish, P.J. Scales, C.Y. Botté, D.L. Callahan, Lipid profile remodeling in response to nitrogen deprivation in the microalgae *Chlorella* sp. (Trebouxiophyceae) and *Nannochloropsis* sp. (Eustigmatophyceae), PloS One 9 (2014) e103389, https://doi.org/10.1371/JOURNAL.PONE.0103389.
[56] W. Wang, K. Freemark, The use of plants for environmental monitoring and assessment, Ecotoxicol. Environ. Saf. 30 (1995) 289–301, https://doi.org/10.1006/EESA.1995.1033.
[57] D. Xu, C. Li, H. Chen, B. Shao, Cellular response of freshwater green algae to perfluorooctanoic acid toxicity, Ecotoxicol. Environ. Saf. 88 (2013) 103–107, https://doi.org/10.1016/J.ECOENV.2012.10.027.
[58] I. Moro, R. Trentin, E. Moschin, F. Dalla Vecchia, Morpho-physiological responses *by Isochrysis galbana* Parke to different concentrations of oxytetracycline, Environ. Pollut. 262 (2020), https://doi.org/10.1016/j.envpol.2020.114273.
[59] P. Chelf, Environmental control of lipid and biomass production in two diatom species, J. Appl. Phycol. 2 (1990) 121–129, https://doi.org/10.1007/BF00023373.
[60] A. Converti, A.A. Casazza, E.Y. Ortiz, P. Perego, M. Del Borghi, Effect of temperature and nitrogen concentration on the growth and lipid content of *Nannochloropsis oculata* and *Chlorella vulgaris* for biodiesel production, Chem. Eng. Process. 48 (2009) 1146–1151.
[61] J.M. Rousch, S.E. Bingham, M.R. Sommerfeld, Changes in fatty acid profiles of thermo-intolerant and thermo-tolerant marine diatoms during temperature stress, J. Exp. Mar. Biol. Ecol. 295 (2003) 145–156, https://doi.org/10.1016/S0022-0981(03)00293-4.
[62] G.Q. Tang, W.P. Novitzky, H. Carol Griffin, S.C. Huber, R.E. Dewey, Oleate desaturase enzymes of soybean: evidence of regulation through differential stability and phosphorylation, Plant J. 44 (2005) 433–446, https://doi.org/10.1111/J.1365-313X.2005.02535.X.
[63] T. Sakamoto, N. Murata, Regulation of the desaturation of fatty acids and its role in tolerance to cold and salt stress, Curr. Opin. Microbiol. 5 (2002) 206–210, https://doi.org/10.1016/S1369-5274(02)00306-5.
[64] M.L. Teoh, S.M. Phang, W.L. Chu, Response of Antarctic, temperate, and tropical microalgae to temperature stress, J. Appl. Phycol. 25 (2013) 285–297, https://doi.org/10.1007/S10811-012-9863-8.
[65] L. Provasoli, Media and prospects for the cultivation of marine algae, in: H. Watanabe, A. Hattori (Eds.), Cultures and Collections of Algae, Proceedings U. S.–Japan Cont., Japanese Society of Plant Physiology, Hakone, 1968, pp. 63–75.
[66] E. Jacob-Lopes, M.I. Queiroz, L.Q. Zepka, Pigments from microalgae handbook, in: Pigments from Microalgae Handbook, 2020, pp. 1–653, https://doi.org/10.1007/978-3-030-50971-2/COVER.
[67] P. Supakorn, Y. Chonlada, S. Anchalee, Pigment production under cold stress in the green microalga *Chlamydomonas reinhardtii*, Agriculture 11 (2021) 564, https://doi.org/10.3390/agriculture11060564.
[68] Y. Zheng, C. Xue, H. Chen, C. He, Q. Wang, Low-temperature adaptation of the snow alga *Chlamydomonas nivalis* is associated with the photosynthetic system regulatory process, Front. Microbiol. 11 (2020) 501355, https://doi.org/10.3389/FMICB.2020.01233/BIBTEX.
[69] S. D'Amico, T. Collins, J.C. Marx, G. Feller, C. Gerday, Psychrophilic microorganisms: challenges for life, EMBO Rep. 7 (2006) 385–389, https://doi.org/10.1038/SJ.EMBOR.7400662.
[70] P. Napaumpaiporn, A. Sirikhachornkit, Effects of high temperature on carotenoid accumulation and gene expression in the model green alga *Chlamydomonas reinhardtii*, Chiang Mai J. Sci. 43 (2016) 452–460.
[71] L.J. Borowitzka, T.P. Moulton, M.A. Borowitzka, The mass culture of *Dunaliella salina* for fine chemicals: from laboratory to pilot plant, in: Eleventh International Seaweed Symposium, 1984, pp. 115–121, https://doi.org/10.1007/978-94-009-6560-7_18.
[72] A. Ben-Amotz, A. Katz, M. Avron, Accumulation of β-carotene in halotolerant alge: purification and characterization of β-carotene-rich globules from *Dunaliella bardawil* (Chlorophyceae), J. Phycol. 18 (1982) 529–537, https://doi.org/10.1111/J.1529-8817.1982.TB03219.X.
[73] A.P. Carvalho, C.M. Monteiro, F.X. Malcata, Simultaneous effect of irradiance and temperature on biochemical composition of the microalga *Pavlova lutheri*, J. Appl. Phycol. 21 (2009) 543–552, https://doi.org/10.1007/S10811-009-9415-Z.